scientific reports

Check for updates

OPEN

Antimicrobial potential of *Citrus australasica* F. Muell. against methicillin-resistant *Staphylococcus aureus* supported by in silico analysis

Esraa M. Mohamed[1,12], Abeer H. Elmaidomy[2,12], Sara Mahmoud Farhan[3], Hesham A. Abou-Zied[4], Ruqaiah I. Bedaiwi[5], Faisal Alsenani[6], Mohamed A. Rabeh[7], Ghada M. Abbas[8]✉, Usama Ramadan Abdelmohsen[9,10]✉ & Mohamed A. Zarka[11]

The prevalence of methicillin-resistant Staphylococcus aureus (MRSA) has been steadily increasing over the past few decades, prompting an urgent need to develop novel antibiotic classes to combat the growing threat of multidrug-resistant bacteria. In this context, a phytochemical investigation of *Citrus australasica* F. Muell. (finger lime, Rutaceae) leaves yielded seven metabolites (1–7), including coumarins and flavonoid glycosides. These compounds were identified as marmin (1), xanthyletin (2), rutin (3), narcissin (4), lactic acid (5), glycerol (6), and *β*-sitosterol (7). The structures of these isolated compounds were elucidated using 1D and 2D NMR. The compounds were evaluated against the MRSA strain (ATCC 33591) using the agar well diffusion method, and compound 1 was the most active. Using a comprehensive protein-protein interaction (PPI) network constructed from the STRING database and visualized using Cytoscape software, we identified key proteins involved in MRSA pathogenesis and potential therapeutic targets. Molecular docking simulations assessed these compounds' binding interactions and affinities with PBP2a, a critical protein in MRSA resistance. Among the tested compounds, marmin exhibited a notable docking score of -6.488 kcal/mol and a low RMSD value of 0.956, indicating a strong and stable interaction. To validate the docking results, molecular dynamics (MD) simulations were conducted to provide insights into the stability and efficacy of these interactions over time. The MD simulations revealed that the protein-ligand complex of PBP2a and marmin (1) maintained stability throughout a 10-nanosecond simulation, with minor fluctuations indicating consistent binding interactions. Based on our findings, the compounds isolated from *C. australasica* showed promise as potential anti-MRSA therapeutic leads for future development.

Keywords *Citrus australasica*, Rutin, MRSA, STRING database, PPI, Docking

Staphylococcus aureus is a common Gram-positive bacterium that can colonize nasal diseases, from mild skin and soft tissue infections to severe and life-threatening conditions, including endocarditis, osteomyelitis, pneumonia, and bacteremia[1]. The widespread misuse of antibiotics has led to the emergence of antibiotic-resistant strains,

[1]Department of Pharmacognosy, Faculty of Pharmacy, MUST, 6th of October City 12566, Giza, Egypt. [2]Department of Pharmacognosy, Faculty of Pharmacy, Beni-Suef University, Beni-Suef 62514, Egypt. [3]Department of Microbiology and Immunology, Faculty of Pharmacy, Deraya University, Minia 61111, Egypt. [4]Department of Medicinal Chemistry, Faculty of Pharmacy, Deraya University, Minia 61111, Egypt. [5]Department of Medical Laboratory Technology, Faculty of Applied Medical Sciences, University of Tabuk, Tabuk, Saudi Arabia. [6]Department of Pharmaceutical Sciences, College of Pharmacy, Umm Al-Qura University, Makkah 21955, Saudi Arabia. [7]Department of Pharmacognosy, College of Pharmacy, King Khalid University, Abha 65251, Saudi Arabia. [8]Department of Pharmacognosy, Faculty of Pharmacy, Horus University- Egypt (HUE), New Damietta 34517, Egypt. [9]Deraya Center for Scientific Research, Deraya University, New Minia 61111, Egypt. [10]Department of Pharmacognosy, Faculty of Pharmacy, Minia University, Minia 61519, Egypt. [11]Department of pharmacognosy, College of Pharmacy, The Islamic University, Najaf, Iraq. [12]Esraa M. Mohamed and Abeer H. Elmaidomy have contributed equally to this work. ✉email: ghabaas@horus.edu.eg; usama.ramadan@mu.edu.eg

including Methicillin-resistant *Staphylococcus aureus* (MRSA)[2]. MRSA develops from the acquisition of the staphylococcal cassette chromosome mec (SCCmec), which harbors the mecA gene responsible for producing an altered penicillin-binding protein 2a (PBP2a). This modified protein has reduced affinity for all β-lactam antibiotics, rendering MRSA resistant to treatment. The significant prevalence of both hospital-acquired MRSA (HA-MRSA) and community-acquired MRSA (CA-MRSA) poses a major global concern. Notably, HA-MRSA is associated with higher mortality rates, prolonged hospitalization, and increased healthcare costs[3].

Vancomycin is often regarded as the last line of defense for treating severe Methicillin-resistant MRSA infections[4]. However, its use is complicated by a range of side effects, including nephrotoxicity, hypotension, and hypersensitivity reactions, which necessitate close monitoring[5]. Consequently, there is an urgent need to identify new alternative anti-MRSA agents with lower toxicity, and one promising approach is using natural products: plant, marine, and endophyte-derived compounds[6–10].

The Citrus genus, part of the Rutaceae family, encompasses 130 genera across seven subfamilies, notable for their significant contributions to fruit and essential oil production. These fruits are a valuable source of Vitamin C, carotenoids, coumarins, folate, and flavonoids, making them a vital diet component. Vitamin C, known for its antiscorbutic properties, is also an antioxidant. The flavonoids in citrus exhibit activities that scavenge hydroxyl radicals and prevent lipid peroxidation. Extensive pharmacological research has aimed to validate the use of Citrus different organs, including seeds and fruit peel, as a versatile medicinal resource, exploring its diverse properties[11–14].

The finger lime (*Citrus australasica* F. Muell.), also known as caviar lime, is one of the six native *Citrus* species found exclusively in Australia[15]. Despite its growing popularity, there is a limited understanding of *C. australasica's* uses and properties[16]. It is mainly used in gourmet cuisine as a garnish or to replace traditional limes in drinks and preserves[17]. The pharmaceutical and cosmetic industries have also expressed interest in the fruit's potential applications[18]. However, most research on Australian *C. australasicas*' chemical and nutritional composition has been conducted on cultivars grown overseas rather than those grown commercially in Australia[19,20]. Previous studies have investigated Australian *C. australasicas*' chemical and nutritional properties, revealing high levels of ascorbic acid and moderate to low levels of antioxidants and phenolics[21,22]. Furthermore, research has identified significant amounts of vitamin E in two- *C. australasica* cultivars[23], and novel volatile compounds have been discovered in the peel of Australian-grown *C. australasica*[24,25].

In this study, seven compounds were isolated and identified from the methanolic extract of the leaves of *C. australasica*. The isolated compounds were subsequently evaluated for their antimicrobial activity against MRSA. Furthermore, molecular docking experiments were performed to investigate the potential mechanisms underlying their activities.

Materials and methods

Plant material

Leaves of *C. australasica* were collected in October 2023 from the Faculty of Pharmacy, Beni-Suef University, Egypt, where permissions were obtained from an appropriate governing body to collect this material. Dr. Abd El-Halim A. Mohammed, a Department of Flora and Phytotaxonomy Research specialist at the Horticultural Research Institute in Dokki, Cairo, Egypt, kindly confirmed the identification. A voucher specimen (2023-BuPD 109) has been deposited at the Department of Pharmacognosy, Faculty of Pharmacy, Beni-Suef University, Egypt.

Chemicals and reagents

The solvents used in this study included n-hexane (b.p. 60–80 °C), dichloromethane, ethyl acetate, n-butanol, ethanol, and methanol, which were sourced from El-Nasr Company for Pharmaceuticals and Chemicals, Egypt. For chromatographic and spectroscopic analyses, deuterated solvents were obtained from Sigma-Aldrich, Saint Louis, Missouri, USA: chloroform-d ($CDCL_3$-*d*), methanol-d4 (CD_3OD-d_4), and dimethyl sulfoxide-d6 (DMSO-d_6). Column chromatography was performed using polyamide, silica gel 60 (63–200 µm) from E. Merck, Sigma-Aldrich, and Sephadex LH20. Silica gel GF254 for thin-layer chromatography (TLC) (El-Nasr Company for Pharmaceuticals and Chemicals, Egypt) was employed for vacuum liquid chromatography. Thin-layer chromatography used pre-coated silica gel 60 GF254 plates (E. Merck, Darmstadt, Germany; 20 × 20 cm, 0.25 mm thick). Spots were visualized by spraying with a para-anisaldehyde reagent (absolute EtOH: sulfuric acid: G.A.A.:*para*-anisaldehyde = 85:5:10:0.5) and then heating to 110 °C[26–32].

Spectral analysis

Nuclear magnetic resonance (NMR) spectra were recorded using a 400 MHz proton NMR and a 100 MHz ^{13}C NMR spectrometer. Tetramethylsilane (TMS) was used as an internal standard in three solvents: $CDCl_3$-*d*, CD_3OD-*d4*, and dimethyl sulfoxide-d6 (DMSO-*d6*). The residual solvent peak was used as a reference for each solvent, with corresponding chemical shifts of ($\delta_H = 7.26$), ($\delta_H = 3.34$, 4.78 and $\delta_C = 49.9$) and ($\delta_H = 2.50$ and $\delta_C = 39.5$) as references respectively. The NMR measurements were performed on two different spectrometers: a Bruker Advance III 400 MHz with a BBFO Smart Probe and a Bruker 400 MHz EON Nitrogen-Free Magnet, both manufactured by Bruker AG in Billerica, Massachusetts, USA. Carbon multiplicities were determined using a DEPT-Q experiment.

Extraction and fractionation of Citrus australasica leaves

200 g of *C. australasica* leaves were ground into a fine powder using an OC-60B/60B grinding machine (60–120 mesh, Henan, Mainland China). The powdered leaves were macerated thrice at room temperature using a 70% ethanol solution (300 mL) over two days. Subsequently, the ethanolic extract was then concentrated under vacuum at 45 °C using a rotary evaporator (Buchi Rotavapor R-300, Cole-Parmer, Vernon Hills, IL, USA) to yield 30 g of crude extract, which was stored at 4 °C for further analysis and phytochemical investigation[30–37].

Isolation and purification of compounds

The total ethanolic extract (30 g) was coarsely fractionated over a polyamide column using gradient elution with water-methanol mixtures starting with (100:0, v/v) till (0:100, v/v), respectively. The effluents, ten mL fraction each, were collected and screened by TLC, and similar fractions were pooled for further study. Six fractions (F1-F6) were collected. Fractions F1 and F2, eluted with water and methanol (8:2, v/v), were purified over Sephadex LH-20 column using methanol (100%). The collected fraction was further purified over silica gel 60 column using gradient elution with dichloromethane and methanol mixtures, starting with 100% dichloromethane till 100% methanol, to yield compounds **5** (20 mg), **6** (30 mg), **7** (10 mg). The polarity of the eluent for each compound is not specified. Fraction F3, which was eluted with a mixture of water and methanol (6:4, v/v), was then purified over Sephadex LH-20 column using isocratic elution with methanol (100%), yielding compounds **3** (12 mg) and **4** (10 mg). Fraction F5, which was eluted with a mixture of water and methanol (2:8, v/v), was further purified over silica gel 60 column followed by Sephadex LH-20 column, to afford compounds **1** (16 mg) and compound **2** (13 mg).

Bacterial strain and growth conditions

The methicillin-resistant Staphylococcus aureus (ATCC 33591) isolate was obtained from a wound infection sample from Minia University Hospital. The bacterial isolate was cultured overnight at 37℃ on Muller Hinton agar (Oxoid, UK). The resulting bacterial suspension was standardized to a turbidity of 0.5 McFarland units, equivalent to approximately 1.5×10^8 CFU/ml[38].

Minimum inhibitory concentration determination

The agar well diffusion method evaluated the isolated compounds' antibacterial activities. The technique was carried out by spreading the microbial inoculum of MRSA across the entire agar surface. The agar plates were prepared as follows: a pure culture of the MRSA strains was grown in nutrient broth at 37 °C for 18–24 h in a shaker incubator until the final concentration was 10^8 CFU/ml (the final concentration was adjusted by sterilized normal saline). Each twenty ml plain nutrient agar was poured into a sterile petri dish. A sterile cork borer punched a six mm well in the solid agar plates under aseptic conditions. Each plate was surface inoculated by 100 µl broth culture of the tested strain in triplicates. Eight serial dilutions of each compound were made (% w/v) in dimethyl sulfoxide (DMSO) (10% aqueous) solvent and sterilized by filtration by passing through a 0.22 µm membrane filter. Plain DMSO was used as a control. 50 µl of each tested dilution was pipetted to the wells of the inoculated agar plates under aseptic conditions. The plates were incubated at 35 °C for 24 h. After incubation, the inhibitory zones were measured in millimeters, and the minimum inhibitory concentration was calculated. Ciprofloxacin was used as a positive control with concentration10mg/ml[38].

In Silico studies

Protein-protein interaction network

To elucidate the molecular interactions pertinent to the antimicrobial properties of *C. australasica* leaf extract, essential phytochemicals identified from empirical studies were entered into the STRING database[36,39–41], a prominent tool for constructing Protein-Protein Interaction (PPI) networks. The focus was on understanding the interactions of these phytochemicals within a human host environment, especially regarding their potential antimicrobial effects against pathogens like MRSA, which are noted for their drug resistance. A rigorous interaction score threshold was maintained, with only interactions scoring above 0.4 included for further analysis. Network visualization and analysis were subsequently conducted using the Cytoscape software[37,42–44], renowned for its robust network analysis capabilities. This step was crucial to pinpoint hub phytochemicals with numerous connections within the network, indicating critical roles in biological processes potentially related to antimicrobial action[7]. Using the CytoHubba/Cytoscape plugin, which specializes in degree-based methods, essential components within the network were identified, highlighting the primary active compounds in the *C. australasica* leaf extract[45]. This analytical approach deepened our understanding of how *C. australasica* phytochemicals interact at the molecular level and highlighted potential targets for enhancing antimicrobial efficacy. Identifying these hub phytochemicals may pave the way for novel therapeutic strategies, particularly in developing more effective treatments against resistant strains of bacteria such as MRSA.

Gene ontology and KEGG pathway enrichment

To explore the roles and molecular interactions of genes associated with MRSA, Gene Ontology (GO) and pathway enrichment analyses were conducted. These analyses offered insights from three perspectives: Biological Processes (BP) detail the involvement of genes in various biological functions; Cellular Components (CC) identify specific cellular locales of gene or protein activity; and Molecular Functions (MF) define precise molecular activities and interactions. Employing ShinyGO (http://bioinformatics.sdstate.edu/go/), a web-based tool renowned for GO analysis, with a rigorous False Discovery Rate (FDR) cutoff of less than 0.05, facilitated the identification of statistically significant gene functions and pathways[46]. The findings were visually represented using enrichment bubble plots generated by SRplot (https://www.bioinformatics.com.cn/en), a tool designed for online data visualization[47]. This methodological approach enhanced the understanding of gene roles and their interactions in MRSA, highlighting key targets for potential therapeutic interventions. This comprehensive analysis underscores the importance of integrating advanced bioinformatics tools in unraveling the complex biological networks associated with MRSA, thereby aiding in the development of effective treatments.

Docking studies

Our study utilized molecular docking, a method simulating the binding interactions between proteins and potential drug molecules, to validate network pharmacology findings. Performed on the Discovery Studio

Client platform, this technique aided in identifying promising drug candidates that could interact effectively with key proteins. Protein structures essential for the study were sourced from the RCSB Protein Data Bank (http://www.rcsb.org/) and prepared. Protein preparation was carried out using UCSF Chimera[48], where all water molecules, ions, and other heteroatoms were removed. Hydrogen atoms were added to the protein structure to ensure proper protonation states at physiological pH, minimizing protonation errors. The polar hydrogens were also optimized, and the overall structure was checked for missing residues or atoms that could impact docking accuracy. The active site residues were identified based on previous studies to ensure accurate docking within the binding pocket[49]. The grid box was centered on the active site with a grid spacing of 0.375 Å (default setting). The grid box center coordinates were set at -11.432 for the x-axis, -9.16 for the y-axis, and 2.636 for the z-axis. The grid dimensions were 60 × 60 × 58 points, covering the full three-dimensional binding pocket of PBP2a, with 431,893 grid points on each map. These parameters ensured comprehensive coverage of the active site during the docking simulations. The energy minimization was performed using the CHARMm force field. The CDOCKER algorithm was configured to generate random ligand conformations. The docking process included simulated annealing steps and evaluation of multiple binding poses to identify optimal interactions. For each ligand, 40 docking runs were performed to ensure thorough sampling of the binding space and to achieve statistically significant results. The top three poses for each ligand were selected based on their binding energy scores. The pose with the lowest binding energy, lowest RMSD, and favorable interactions with key active site residues were selected for subsequent molecular dynamics simulations[33,34,50–54]. This streamlined approach confirmed our network analysis and highlighted effective drug candidates.

Molecular dynamics simulation

A molecular dynamics (MD) simulation was carried out to validate the docking results using GROMACS 2021[55]. The protein of interest was prepared with UCSF Chimera[48], which included the addition of hydrogen atoms. Two force fields were utilized: Charm 36 for the protein and CGenFF for the ligands[56]. The entire complex was solved in a water box with a TIP3P water model, ensuring a minimum extension of 1 nm in all directions. The system was balanced by adding Sodium chloride ions for neutralization and further supplemented to a final concentration of 150 mM. Initial minimization used the steepest descent method, followed by 100 ps of NVT and NPT equilibration phases at 300 K and 1.0 bar, respectively, with position restraints maintained on the protein and ligands. Finally, a 10-ns production run was performed with position restraints removed, capturing trajectories every 10 ps for subsequent RMSD and binding energy analyses. This comprehensive setup provided a robust framework for confirming the molecular interactions and stability of the proposed drug candidates against MRSA.

Statistical analysis

The data were tabulated using the statistical program GraphPad Prism version-9 (GraphPad, La-Jolla, CA, USA).

Results and discussion

Phytochemical Investigation of Citrus australasica leaves

Based on the physicochemical and chromatographic plots, the spectral investigations from UV, ^{1}H, and DEPT-Q NMR, besides correlations with the literature and some authoritative samples, the crude methanolic extract of *C. australasica* leaves were found to contain the known compounds marmin (**1**)[57], xanthyletin (**2**)[58], rutin (**3**)[59], narcissin (**4**)[60], lactic acid (**5**)[61], glycerol (**6**)[62], and *β*-sitosterol (**7**)[63], (Figures S1-11, Fig. 1).

Anti MRSA Activity of Citrus australasica leaves isolated compounds

In this investigation, the isolated compounds from *C. australasica* leaf methanolic extract (1–6) were evaluated for their anti-MRSA activity using the agar well diffusion method (Table 1). Notably, compound **1** was the most active, showing strong anti-MRSA activity comparable to ciprofloxacin as a control drug.

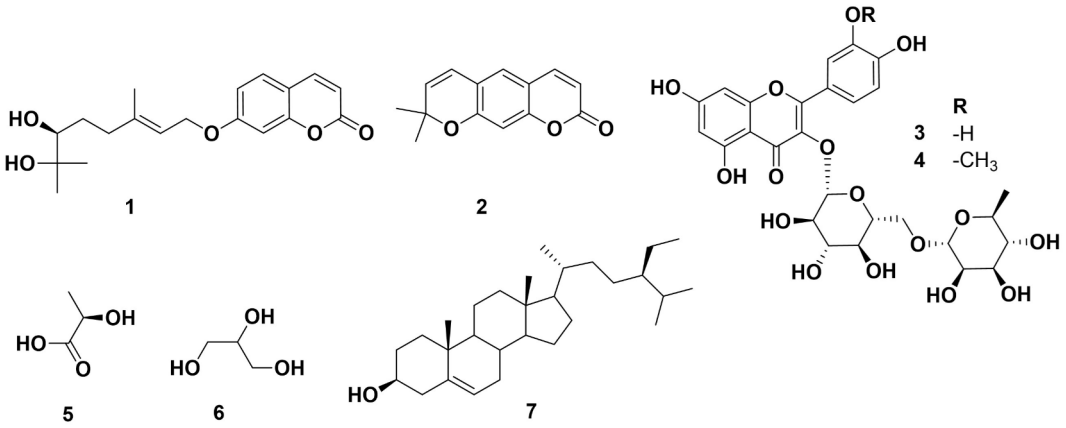

Fig. 1. Structures of compounds isolated from *Citrus australasica* leaves.

Compounds	MIC (mg/mL)	Ciprofloxacin MIC (mg/mL)
1	0.1	0.512
2	0.7	0.512
3	0.3	0.512
4	0.5	0.512
5	0.4	0.512
6	0.6	0.512

Table 1. The anti-MRSA activity of *Citrus australasica* leaves isolated compounds using the agar well diffusion method.

GraphPad Prism 9 software calculated the minimum inhibitory concentration MIC (mg/mL) values. The concentration of each pure compound was transformed to log10. All experiments were performed at least two times. $^{*}p < 0.05$, Student's *t*-test.

Protein-protein interaction network

Therapeutic targets for MRSA infections

Based on our experimental findings, a dataset of 72 target proteins associated with MRSA (Methicillin-resistant **Staphylococcus aureus**) infections was meticulously curated from the NCBI-GEO and PharmGKB databases. These proteins, detailed in supplementary **Table S1**, include critical targets and biomarkers central to our investigations into MRSA. This collection highlights the importance of these proteins in the context of MRSA infections and strengthens their potential as therapeutic targets, supported by experimental evidence from our research efforts.

STITCH database correlation of MRSA targets and Citrus australasica compounds

In this comprehensive analysis, we employ the STITCH database with precision to investigate the interactions between key active components in *C. australasica*, specifically, glycerol, lactate, rutin, narcissin, and sitosterol—and protein targets cataloged in GEO and PharmGKB (Fig. 2). This initiative is crucial for advancing our goal to delve into the antimicrobial effects of *C. australasica* isolated compounds against MRSA infections. The analysis sheds light on the synergistic potential of the *C. australasica* isolated compounds. The observed synergy indicates a sophisticated interaction between the combined bioactive molecules in the *C. australasica* isolated compounds and proteins related to MRSA. This interplay is believed to enhance the overall efficacy of the isolated compounds, broadening their therapeutic capabilities against MRSA infections.

Protein network construction for MRSA interaction with citrus australasica compounds

For the development of the Protein-Protein Interaction (PPI) network in our study, proteins relevant to MRSA and the active components found in *C. australasica* leaves were incorporated into the STRING database, version 12.0 (https://string-db.org/cgi/input?sessionId=barlI0uOHF46), to construct preliminary PPI networks elucidating their direct and functional associations. This process facilitated the visualization of the PPI network diagram through Cytoscape software, version 3.10.1. Utilizing the Cytoscape Analyzer feature, we established an extensive protein interaction network comprising 90 nodes and 1857 interaction linkages, which resulted in an average node connectivity of 41.27. The complexities of this network are detailed in Fig. 3, highlighting the comprehensive analysis of protein interactions pertinent to our study on the antimicrobial effects of *C. australasica* leaves isolated compounds against MRSA infections.

Analysis of overrepresented gene ontology terms

The Gene Ontology (GO) enrichment analysis for the current study on the antimicrobial effects of *C. australasica* leaves isolated compounds against MRSA was conducted using ShinyGO v0.80. Our findings demonstrate the significant involvement of proteins in Biological Processes (BP) such as "Innate immune response" and "Humoral immune response," which are crucial for the defense against MRSA infections. In the Cellular Component (CC) category, terms like "Extracellular vesicle" and "Membrane attack complex" indicate the targeted cellular locations where *C. australasica* compounds might exert antimicrobial effects. The Molecular Function (MF) category, with terms like "Endopeptidase inhibitor activity" and "Complement binding," suggests that these proteins may engage in signaling pathways that disrupt MRSA mechanisms. These findings align with our aim to delineate the molecular mechanisms through which *C. australasica* leaves compounds confer protection against MRSA. The detailed results and implications are presented in Supplementary **Table S2**, which documents the statistically significant GO terms and their relevance. The visual representations in Fig. 4 display the enhanced Gene Ontology (GO) terms across the categories of Biological Process (BP), Cellular Component (CC), and Molecular Function (MF).

Examination of predominant KEGG pathways

The KEGG pathway analysis is crucial for our study, linking the molecular actions of *C. australasica* leaves compounds to specific biological pathways affected by MRSA infections[64–66]. Our data, detailed in supplementary **Table S3**, are illustrated in a bar plot (Fig. 5) and show significant enrichment in pathways such as "*Staphylococcus aureus* infection" and "Complement and coagulation cascades." These pathways are vital for understanding how

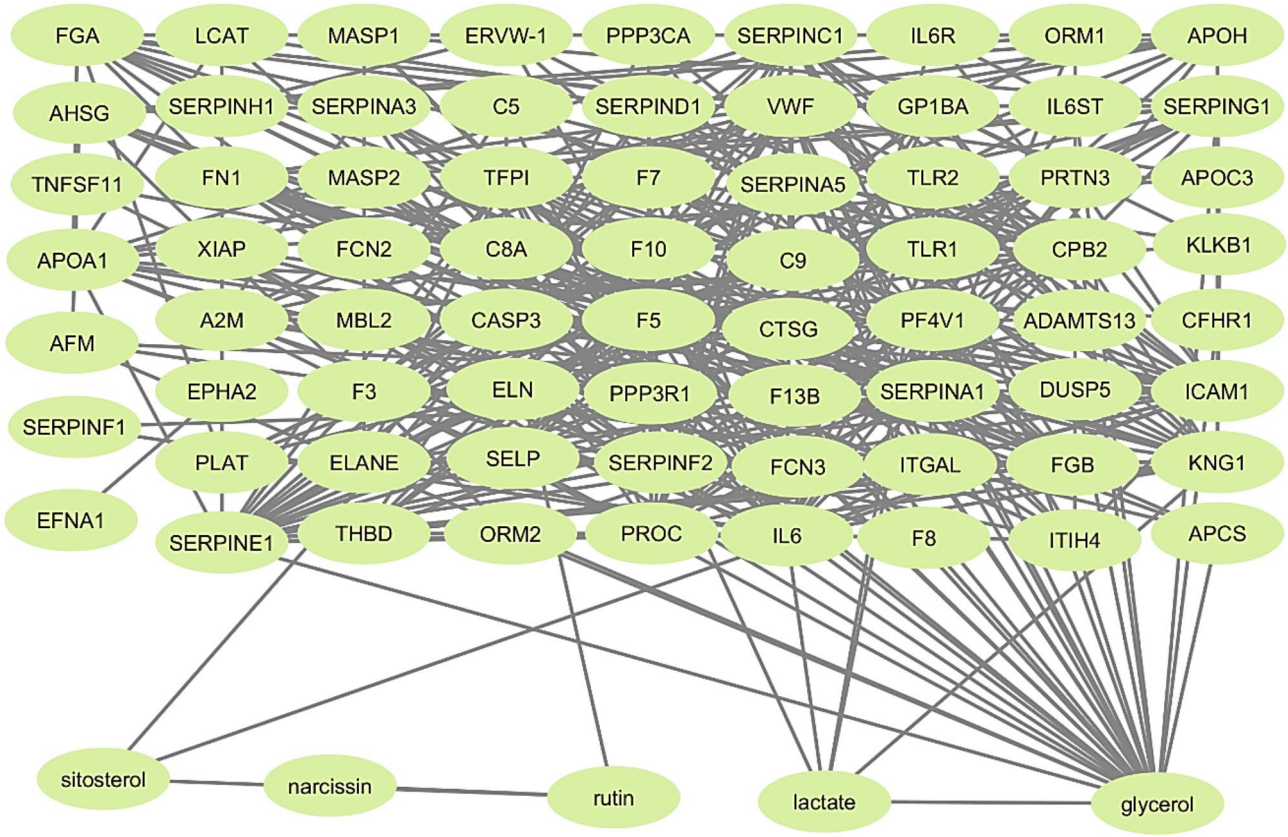

Fig. 2. STITCH analysis of MRSA targets and key active compounds in *Citrus australasica* isolated compounds from leaves.

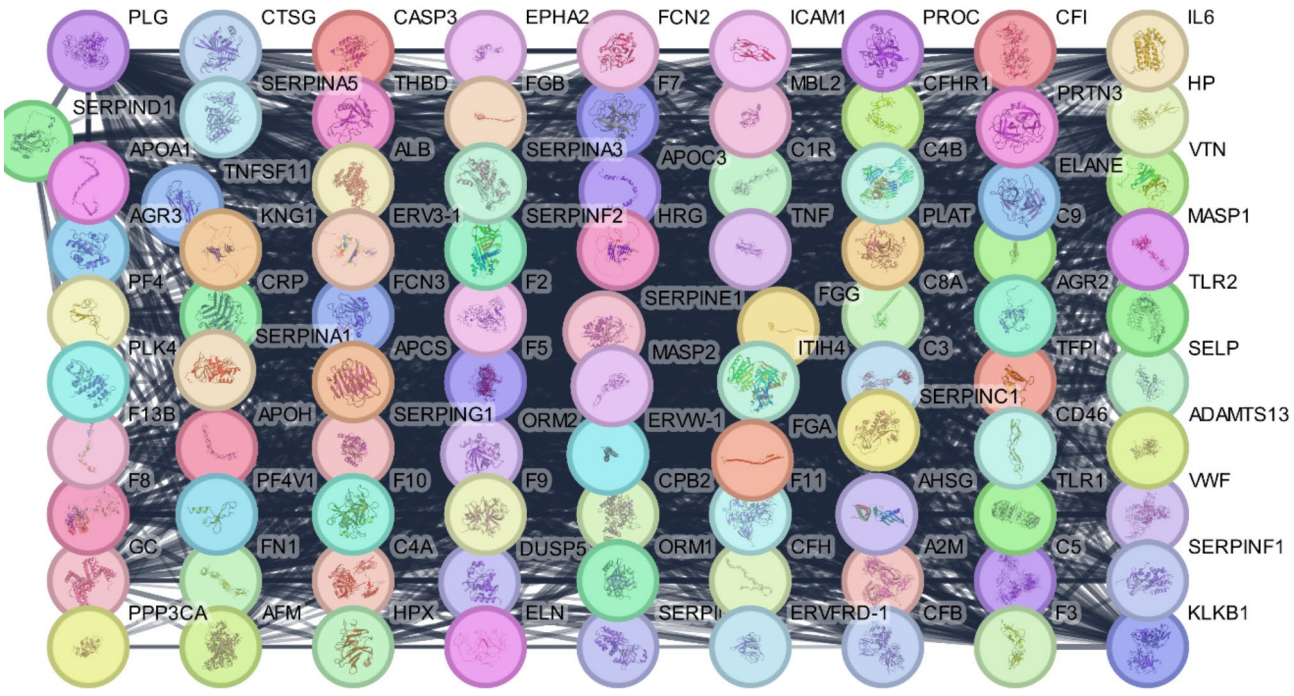

Fig. 3. PPI network for *Citrus australasica* leaves against MRSA infections.

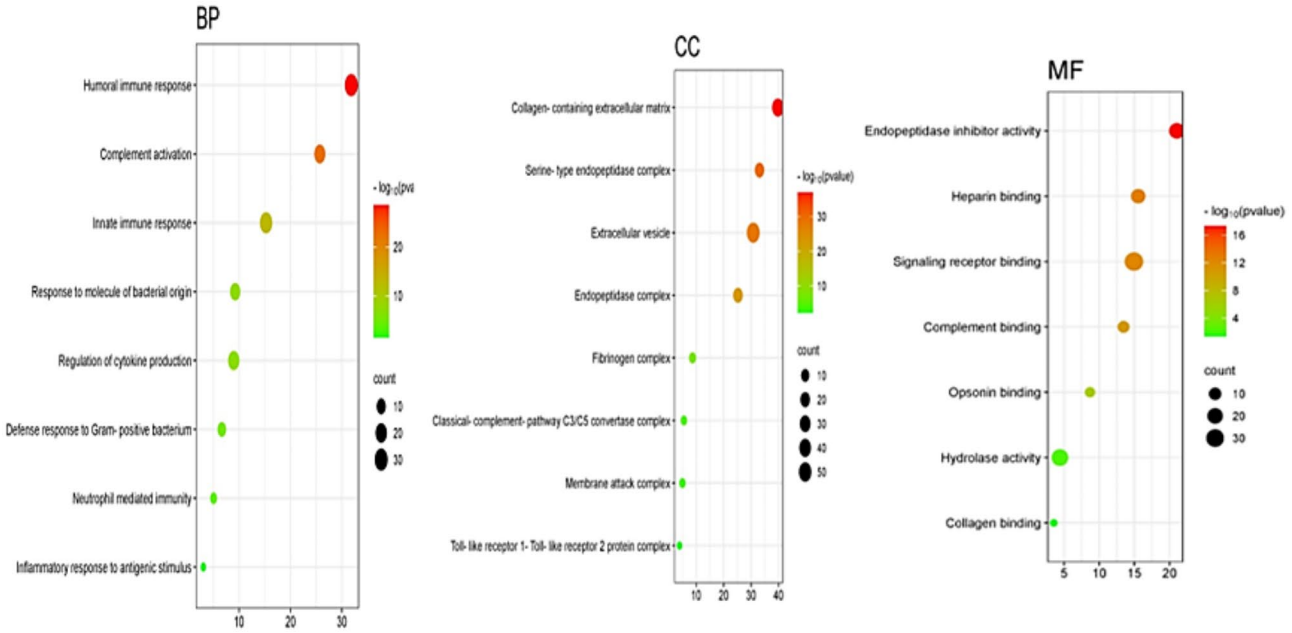

Fig. 4. The bubble chart illustrates the gene ontology of target genes affected by MRSA infections related to identified compounds from *Citrus australasica* leaves: (BP) Biological Process, (CC) Cellular Component, and (MF) Molecular Function.

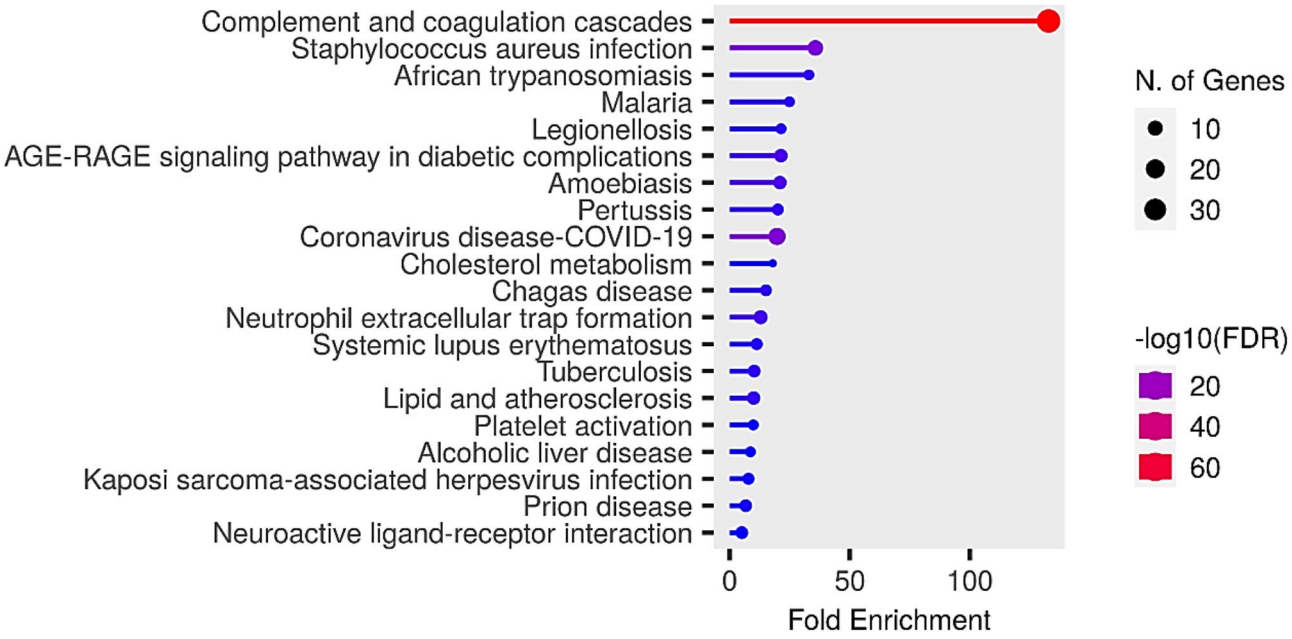

Fig. 5. KEGG pathway enrichment analysis of target genes affected by MRSA infections related to identified compounds from *Citrus australasica* leaves[64–66].

the bioactive components in *C. australasica* leaves might influence gene expression and protein interactions to combat MRSA infections, highlighting potential mechanisms of antimicrobial action and therapeutic targets for intervention against MRSA.

In our study, the KEGG pathway analysis focusing on "*Staphylococcus aureus* Infection" highlights the potential molecular targets affected by *C. australasica* compounds in combating MRSA infections. Key elements such as complement and coagulation cascade, surface proteins' role, and opsonization inhibition have been identified (Fig. 6). These pathways are crucial for understanding how MRSA manipulates host responses to promote its survival and proliferation and how *C. australasica* might counteract these mechanisms. Identifying

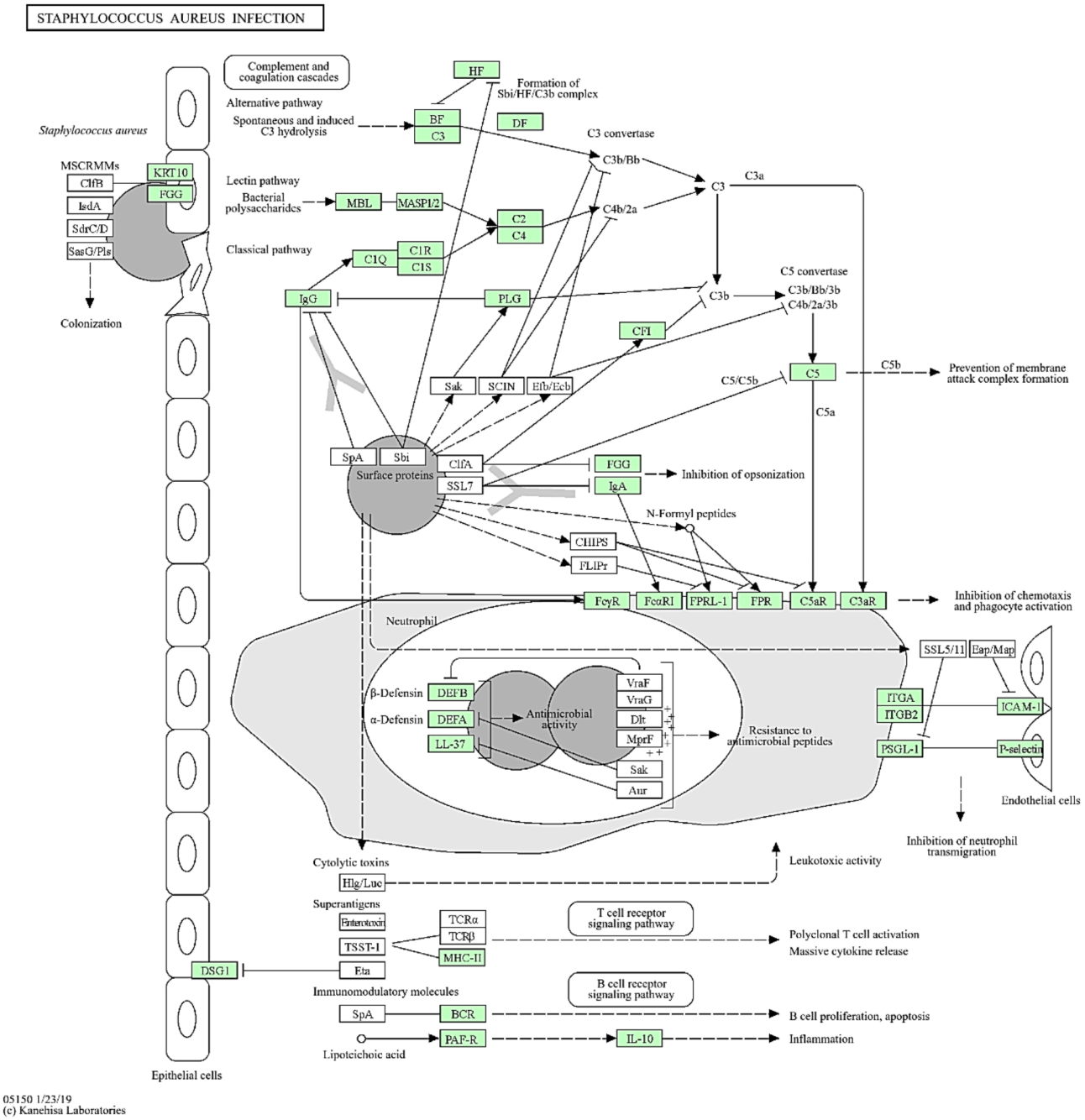

Fig. 6. Pathways commonly exploited by MRSA to evade immune responses[64–66].

these pathways provides insight into the antimicrobial mechanisms of *C. australasica* leaf compounds, suggesting that it may exert protective effects by modulating pathways commonly exploited by MRSA to evade immune responses. This underscores the potential of *C. australasica* as a natural source for developing new therapeutic strategies against MRSA infections, enhancing our understanding of its bioactive roles in disrupting the infection cycle at a molecular level.

Identification of central hub Genes in MRSA interaction with citrus australasica compounds

The CytoHubba plugin identified essential hub genes within the PPI network related to the antimicrobial effects of *C. australasica* against MRSA. These hub genes, including CRP, C3, VWF, SERPING1, and FGA, demonstrate high connectivity and are of significant interest (Fig. 7). These genes play crucial roles in the immune response and coagulation processes. **CRP (C-reactive protein)** is a marker of inflammation and has roles in opsonization and activating complement pathways that enhance the immune system's ability to fight infections. **C3 (Complement component 3)** is central to activating the complement system, which aids in clearing pathogens like MRSA. **VWF (von Willebrand factor)** assists in blood coagulation and the initial stages of wound healing but also

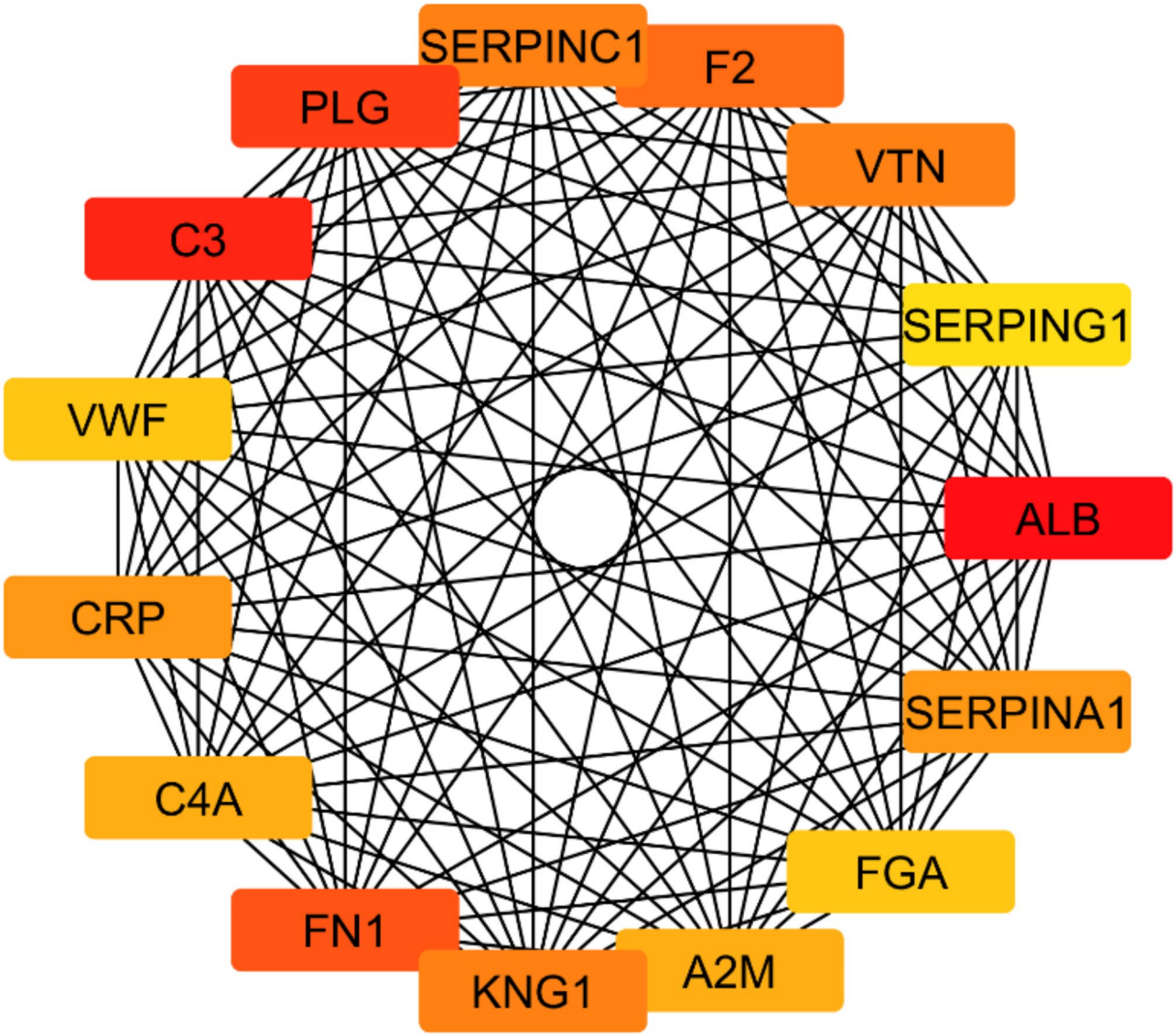

Fig. 7. Top hub genes associated with the antimicrobial effects of *Citrus australasica* against MRSA infections, identified through network pharmacology analysis. These genes are critical targets linked to MRSA resistance mechanisms, supporting the potential of bioactive compounds from *Citrus australasica* in combating MRSA infections.

has roles in immune responses. **SERPING1 (C1 inhibitor)** regulates the complement and contact system to prevent excessive inflammation and tissue damage. **FGA (Fibrinogen alpha chain)** is involved in clot formation and cellular interactions during the immune response. These interactions suggest a dynamic reaction to MRSA infection, highlighting how *C. australasica* components might influence these pathways. The antimicrobial strategy of *C. australasica* could involve enhancing innate immunity through modulation of complement activity and acute phase responses, potentially disrupting MRSA's ability to evade the host immune system. This comprehensive understanding of protein interactions aids in pinpointing therapeutic targets for more effective treatment strategies against MRSA infections.

Penicillin-binding protein 2a (PBP2a) is a critical component in the resistance mechanism of MRSA, providing the bacteria with the ability to resist beta-lactam antibiotics, such as penicillins and cephalosporins. PBP2a, encoded by the mecA gene, alters the regular binding targets of beta-lactams, allowing for cell wall synthesis even in the presence of these antibiotics. Activation of the complement system, where C3 plays a central role, can enhance the immune system's ability to clear pathogens, including MRSA. The complement system could potentially facilitate the clearance of bacteria regardless of the presence of PBP2a, as it involves membrane attack complexes that lyse cells independently of the peptidoglycan synthesis inhibited by PBP2a.

Molecular modeling with PBP2a (penicillin binding protein 2a)

To elucidate the mechanism underlying the antimicrobial effects of the isolated compounds, we performed molecular docking studies using **PBP2a** (Penicillin-Binding Protein 2a) from *MRSA* as the target. The rationale for selecting **PBP2a** lies in its critical role in MRSA resistance to β-lactam antibiotics. The low affinity of PBP2a for these antibiotics is the primary cause of resistance in MRSA strains, making it a prime target for potential inhibitors. Previous studies have successfully used this structure to model interactions with antimicrobial agents, further validating its relevance for this investigation. The crystal structure of PBP2a used in this study corresponds to chain A, with a resolution of 1.8 Å, as retrieved from the Protein Data Bank (PDB ID: 1VQQ). The resolution of this structure provides a high level of detail regarding the atomic coordinates of the protein. The associated **R-factor** is **0.237**, indicating a good fit between the observed and calculated data from X-ray diffraction experiments[67,68]. The active site was selected based on previous research and verified using structural visualization tools[49]. The molecular docking study conducted in this research utilized flexible docking to account for receptor flexibility during ligand interactions, thereby improving the accuracy of docking predictions. The residues were softened during the docking process by applying torsional degrees of freedom, allowing them to adjust their conformations in response to ligand binding. The protein structure was prepared using PyMOL version 1.5.0.3 to remove water molecules and heteroatoms[69]. The molecular docking study conducted in this research utilized flexible docking to account for receptor flexibility during ligand interactions, thereby improving the accuracy of docking predictions. The docking protocol was validated using a docking experiment with the reference drug ciprofloxacin. Ciprofloxacin was docked into the active site of PBP2a using the same docking protocol to assess its binding performance as a reference. The root mean square deviation (RMSD) between the docked pose and the predicted binding interactions was calculated. RMSD value was 2.0 Å, and the docking score was −6.7 kcal/mol. This validation step confirmed the accuracy and reliability of the docking method. The docking pose of ciprofloxacin revealed strong interactions within the PBP2a binding site, including hydrogen bonds with residues such as Glu239 and Thr216, salt bridge interactions with Arg241, and hydrophobic interactions with SER240. Its binding affinity, reflected by a docking score of -6.7 kcal/mol, highlights its effectiveness in binding to the active site (Fig. 8).

The docking simulations between essential compounds from *C. australasica* leaves (**Compounds 1–7**) and Penicillin-binding protein 2a (PBP2a) of MRSA aimed to identify potential binding affinities, key interaction points, and the overall feasibility of these compounds to act as competitive inhibitors of PBP2a, thereby possibly restoring the effectiveness of beta-lactam antibiotics against MRSA. Seven compounds were screened for their ability to bind to PBP-2a, with the docking results detailed in Supplementary **Table S4**. When performing molecular docking studies, two key parameters are used to assess the effectiveness of a compound: the **S Score** (docking score) and **Root Mean Square Deviation (RMSD)**. The **S Score** reflects the **binding affinity** between a compound and the target protein, with more negative values indicating stronger binding. **Marmin** (1)had

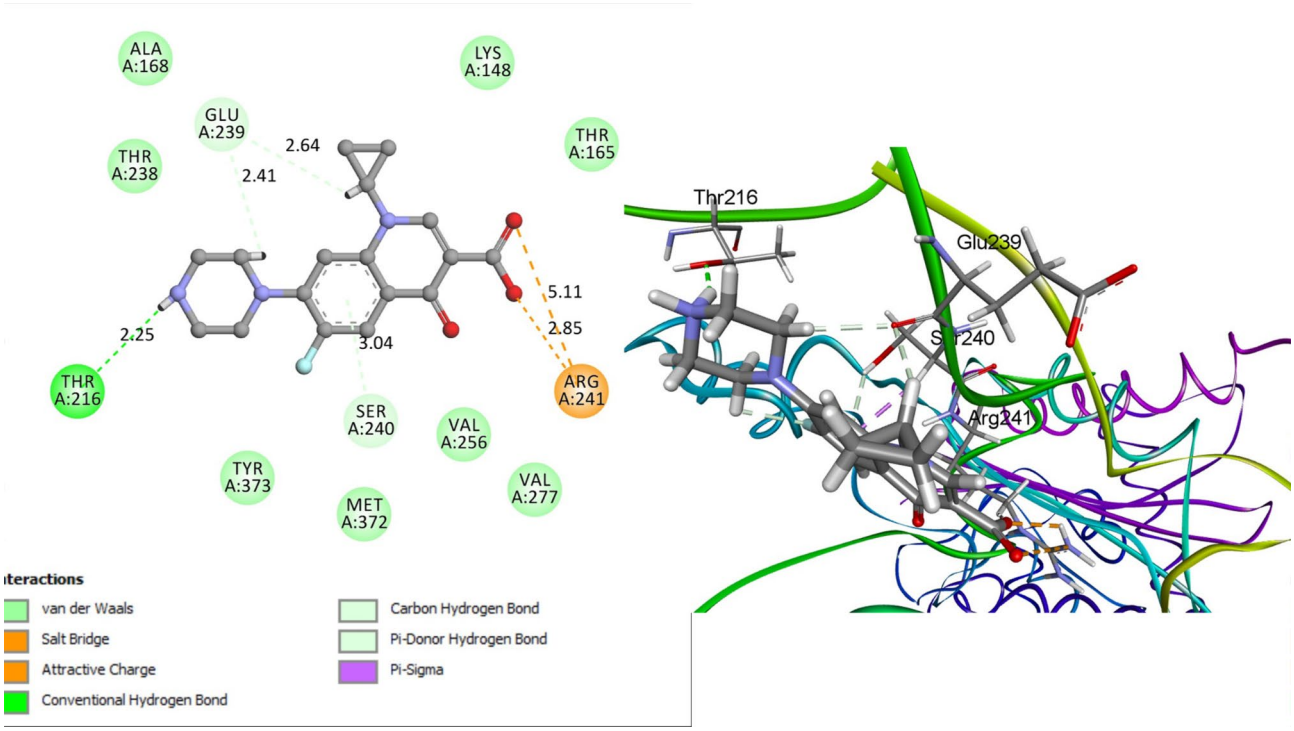

Fig. 8. Two-dimensional and three-dimensional interaction diagrams of ciprofloxacin within the binding pocket of PBP2a (PDB ID: 1VQQ), showing key binding interactions. Ciprofloxacin serves as a positive control in the docking study, highlighting hydrogen bonds with Thr216 and Glu239, salt bridge interactions with Arg241, and hydrophobic contacts with Ser240.

an S score of **-6.488 kcal/mol**, showing strong binding to PBP2a. **Narcissin** had the most negative S score at **-6.513 kcal/mol**, indicating it binds even more tightly than marmin. The **RMSD** suggests the stability of the compound within the protein's binding site. A lower RMSD value suggests a more stable interaction, meaning the compound stays consistently bound to the protein. **Marmin** had the **lowest RMSD (0.956 Å)**, suggesting it binds stably to PBP2a. **Narcissin** (4), despite its better docking score, had a higher RMSD of **1.531 Å**, indicating less stability than marmin. While narcissin had a slightly better docking score, marmin was selected as the best candidate due to its favorable balance between **binding solid affinity (-6.488 kcal/mol)** and **stable binding pose (RMSD of 0.956 Å)**. This combination suggests that marmin binds well and remains stably bound within the PBP2a active site, making it the most likely to be an effective inhibitor. Other compounds, such as xanthyletin (2) and rutin (3), exhibited docking scores of **-5.124 kcal/mol** and **– 6.014 kcal/mol**, respectively. **Compound 1** (marmin) displayed several meaningful interactions contributing to its stable binding within the active site. The 2D interaction diagram highlights fundamental interactions between Marmin and surrounding residues of PBP2a. Specifically, Marmin forms a conventional hydrogen bond (2.09 Å), depicted by green dotted lines, with residue **Thr216**, stabilizing the compound within the active site. In addition to hydrogen bonding, Marmin engages in hydrophobic interactions with residues such as Val256 (5.47 Å), Arg241 (4.92 Å), and Val277(4.66 Å), shown as pink arcs in the diagram, indicating stabilization of the aromatic ring structure of Marmin within the binding pocket as detailed in Fig. 9. The compound is oriented in the 3D interaction diagram, So its aromatic ring structure is deeply embedded, interacting with critical residues. These interactions, crucial for binding affinity, were visually detailed in Fig. 9. Compared to the reference compound ciprofloxacin, Marmin shares overlapping binding interactions, suggesting that Marmin could serve as a competitive alternative inhibitor. These findings highlight its potential as a leading candidate for the development of new antibacterial agents to combat MRSA infections.

Molecular dynamics simulation with PBP2a (penicillin binding protein 2a)

Thus, the antimicrobial activity of **compound 1** from *C. australasica* against MRSA might involve interaction with penicillin-binding protein 2a (PBP-2a). This hypothesis is further explored using molecular dynamics simulations to assess the stability and efficacy of these interactions over time. By examining the dynamic behavior of compound **1** when bound to PBP-2a, we aim to uncover potential mechanisms through which *C. australasica* compounds might inhibit the critical resistance mechanism in MRSA, offering a promising avenue for developing novel antibacterial therapies. The Root Mean Square Deviation (RMSD) analysis was conducted on the molecular dynamics (MD) trajectory of Penicillin Binding Protein 2a (PBP-2a) from MRSA, complexed with Compound 1 from *C. australasica* leaves. After aligning the alpha carbons to the minimized structure, this analysis provides insights into the stability of the protein-ligand complex throughout the simulation. As depicted

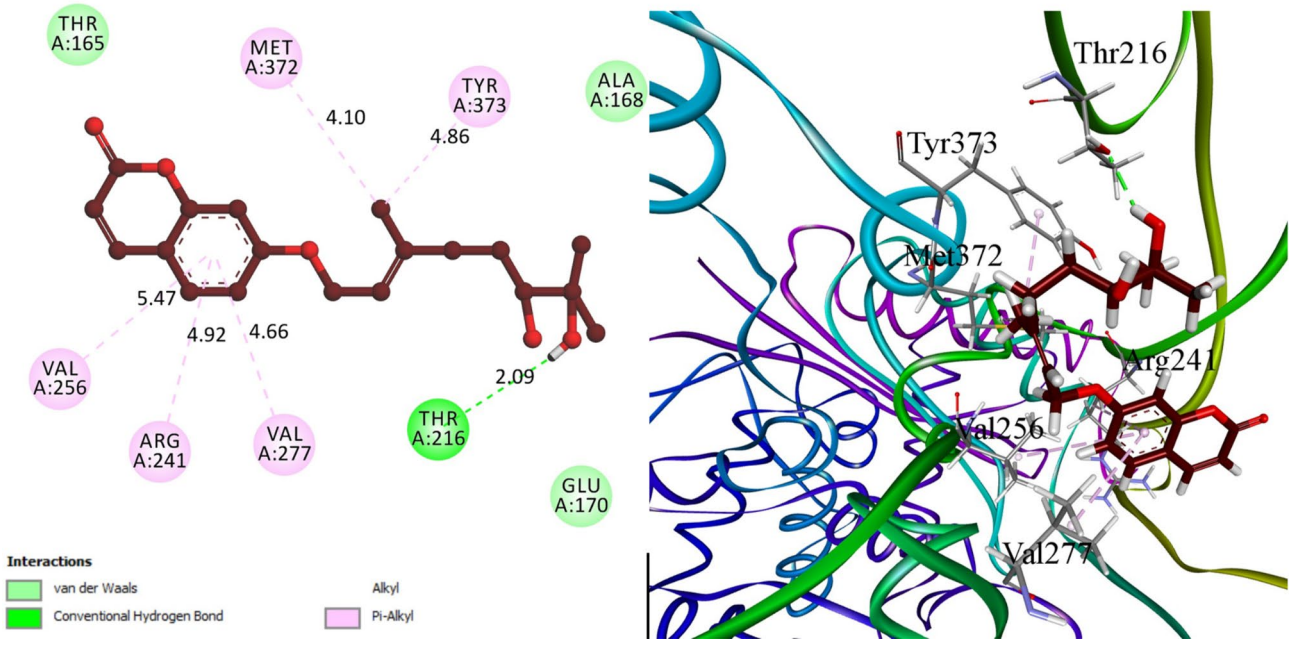

Fig. 9. Two-dimensional and three-dimensional interaction diagrams of Compound 1 (Marmin) within the binding pocket of PBP2a (PDB ID: 1VQQ). The diagrams highlight key binding interactions, including a hydrogen bond with Thr216 (2.09 Å) and hydrophobic interactions with Val256 (5.47 Å), Arg241 (4.92 Å), and Val277(4.66 Å).

in Fig. 10, the RMSD values fluctuate throughout 10 nanoseconds, demonstrating the dynamic nature of this interaction. Initially, the RMSD rapidly stabilizes, indicating that the complex reaches a stable conformation early in the simulation. The RMSD exhibits minor fluctuations, suggesting the ligand consistently interacts with PBP-2a. This stability is crucial as it reflects the potential efficacy of Compound 1 to serve as a basis for developing new antimicrobial agents against MRSA by targeting the critical resistance mechanism mediated by PBP-2a.

The Root Mean Square Fluctuation (RMSF) of individual atoms in the MRSA Penicillin Binding Protein 2a (PBP-2a) complexed with **Compound 1** derived from *C. australasica* leaves. The RMSF values are plotted against the atom indices, ranging from 0 to 10,000, showing the dynamic flexibility across the protein structure during the molecular dynamics simulation. Peaks in the graph indicate regions of higher flexibility within the protein, which may correspond to active sites or regions involved in binding interactions with the ligand. This data is crucial for identifying potential flexibility or stability issues within the protein-ligand complex, helping to elucidate the molecular interactions that underpin the potential antimicrobial effectiveness of **Compound 1** against MRSA (Fig. 11).

Several hydrogen bonds formed between MRSA Penicillin Binding Protein 2a (PBP-2a) and Compound 1 from *C. australasica* leaves were studied throughout a 10-nanosecond molecular dynamics simulation. The hydrogen bond count is an essential indicator of the stability and specificity of the protein and ligand interaction. The fluctuation in the number of hydrogen bonds over time, as shown, highlights the dynamic nature of this interaction. Periods of increased hydrogen bonding, observed in the peaks of the plot, suggest more robust interaction phases, which may correspond to higher stability or binding affinity of the compound towards the protein (Fig. 12).

Lennard-Jones (short-range) energy fluctuations of the MRSA Penicillin Binding Protein 2a (PBP-2a) when complexed with **Compound 1** derived from *C. australasica* leaves throughout a 10 nanosecond molecular dynamics simulation. The energy values, measured in kilojoules per mole (kJ/mol), indicate the strength of the non-bonded interaction between the protein and the compound. As depicted, the energy levels show considerable variation over time, reflecting the dynamic interactions and stability within the complex (Fig. 13). These fluctuations are essential to understanding how **Compound 1** influences the structural integrity and

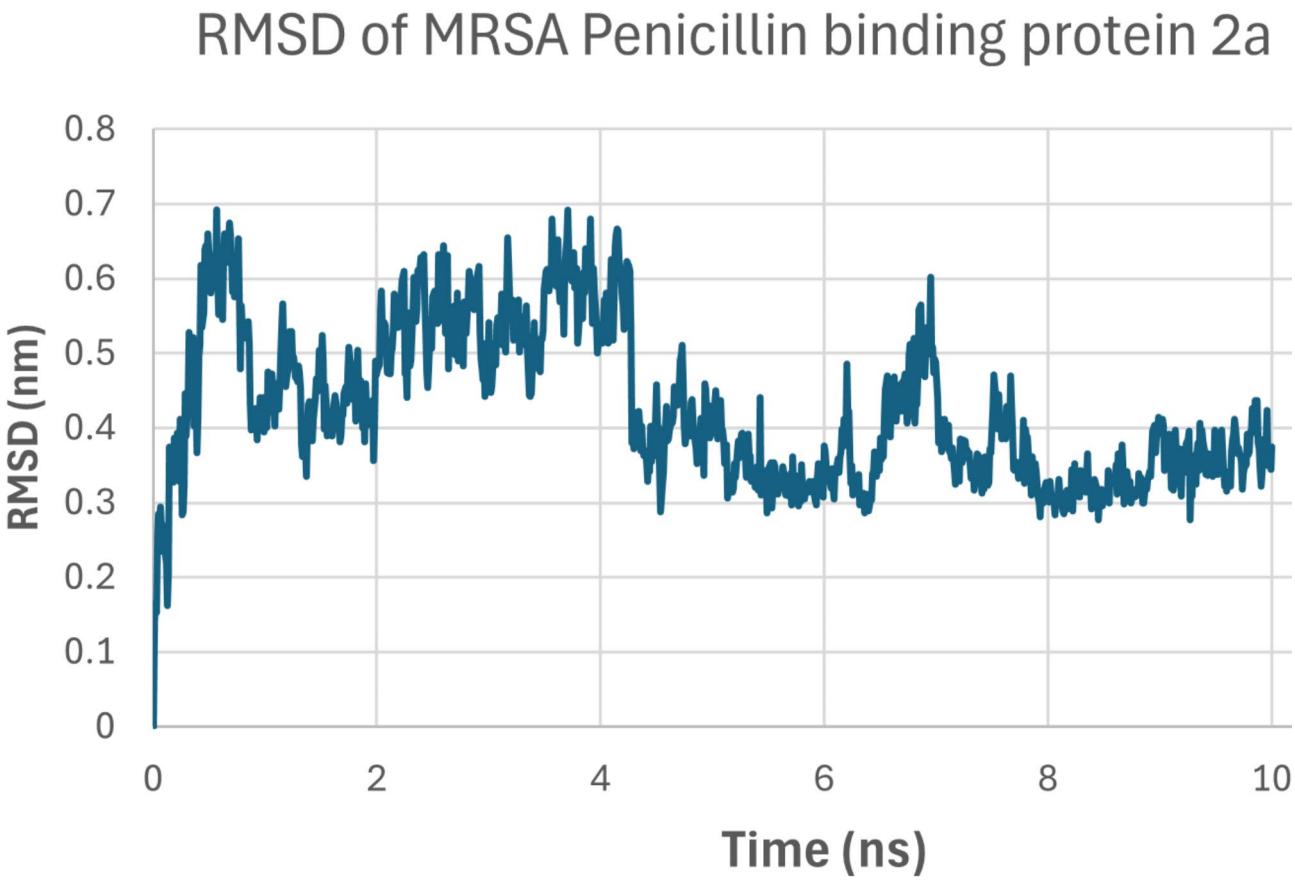

Fig. 10. Root Mean Square Deviation (RMSD) analysis of the MRSA Penicillin-Binding Protein 2a (PBP2a) complexed with Marmin, a compound isolated from *Citrus australasica* leaves, over 10 ns molecular dynamics simulation. The RMSD plot reflects the structural stability of the protein-ligand complex, indicating that Marmin forms a stable interaction with PBP2a, which supports its potential as an effective inhibitor to combat MRSA infections.

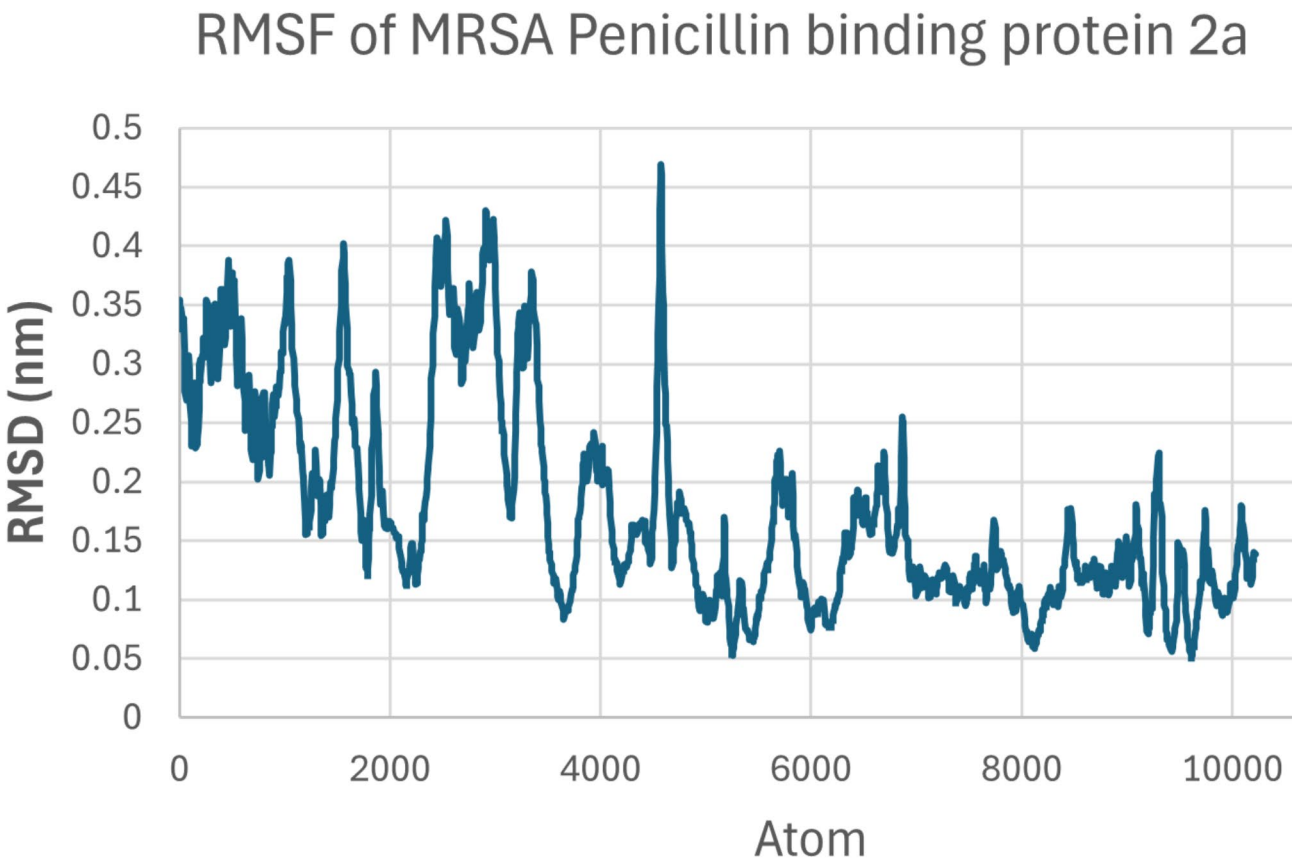

Fig. 11. Root Mean Square Fluctuation (RMSF) analysis of MRSA Penicillin-Binding Protein 2a (PBP2a) in complex with Marmin, a compound isolated from *Citrus australasica* leaves. The RMSF plot highlights fluctuations of individual amino acid residues during the molecular dynamics simulation, indicating key flexible regions of the protein-ligand complex and providing insights into the stability and dynamic behavior of the binding interactions.

function of PBP-2a, providing insights into its potential as a therapeutic agent against MRSA by disrupting the bacterium resistance.

These analyses collectively underscore the potential of **Compound 1** as a viable candidate for inhibiting the PBP-2a enzyme, which is crucial for the resistance mechanism in MRSA. Thus, Compound 1 offers a promising therapeutic pathway against MRSA infections.

Conclusion

The findings of this study demonstrated that seven compounds were isolated from *C. australasica* leaves extract, and compound **1** exhibited a high in vitro anti-MRSA activity. The Protein-Interaction network analysis identified TLR2, VWF, and TNF as central hub genes. Marmin (**1**) showed the most promising results with a notable docking score of -6.488 kcal/mol and a low RMSD value of 0.956, suggesting a strong and stable interaction with PBP2a. The MD simulations demonstrated that the PBP2a-marmin (1) complex remained stable during the 10-nanosecond simulation, with RMSD and RMSF analyses confirming consistent binding interactions. Hydrogen bond analysis and Lennard-Jones energy profiles indicated favorable and stable non-bonded interactions. These observations suggest that these compounds, particularly compound **1**, hold promise as potential MRSA treatment. However, further investigations are necessary to elucidate these compounds' cellular mechanisms of action. Studies using techniques such as proteomics and transcriptomics could reveal specific cellular pathways that are affected by these compounds. Also, the derivatization of the isolated compounds may improve binding affinity and reduce side effects. Moreover, conducting studies on a wider range of MRSA strains, including those with varying resistance profiles, would provide valuable insights into the efficacy of these compounds in diverse clinical scenarios. Assessing the potential synergistic effects of the compounds when used in combination with standard antibiotics, especially β-lactams could enhance treatment options, particularly in cases of multi-drug-resistant infections. This approach may help to lower the required doses of existing antibiotics and reduce the likelihood of resistance development. Exploring the encapsulation of *C. australasica* metabolites in nanoformulations could significantly enhance their stability, bioavailability, and targeted delivery to sites of infection. Nanoparticles can facilitate better penetration of bacterial biofilms and enhance the antimicrobial effects of the metabolites.

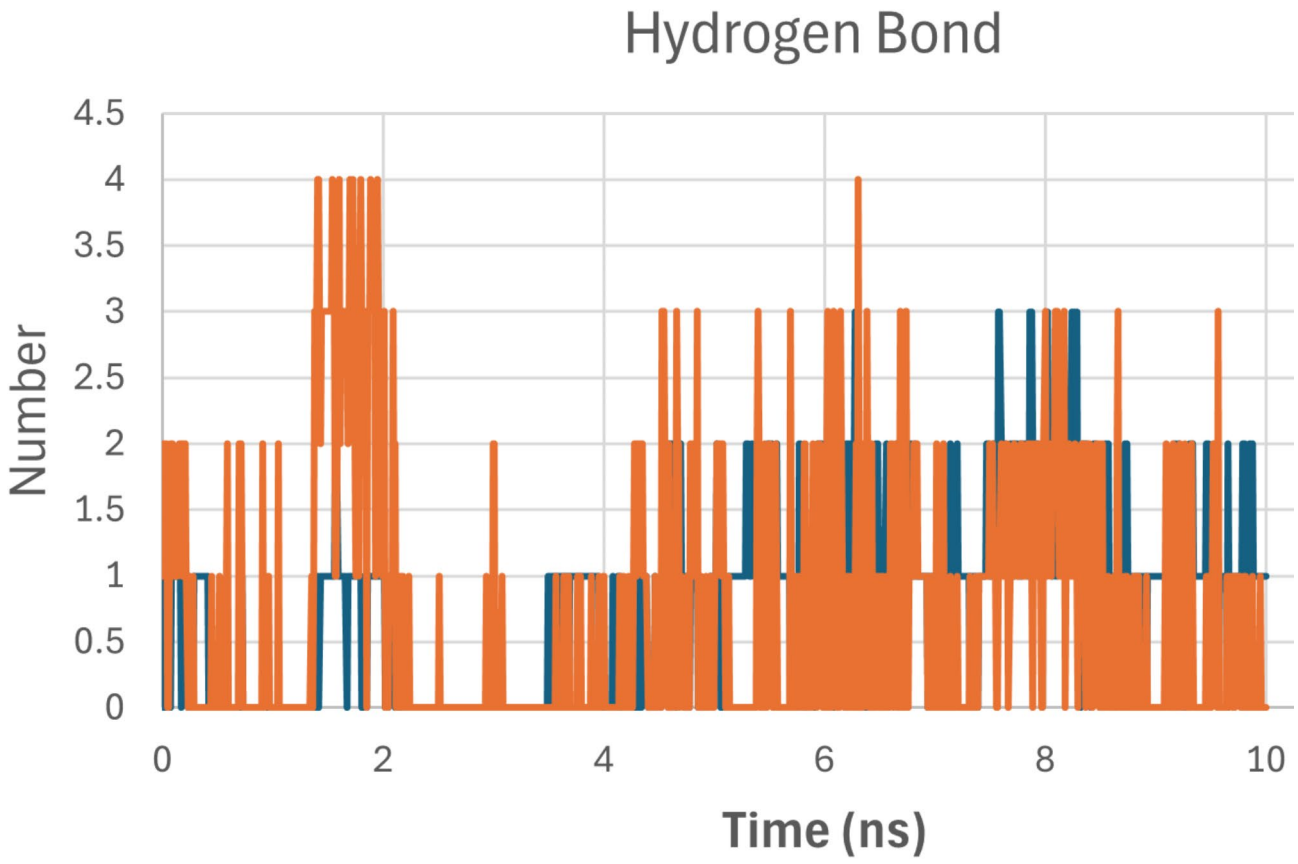

Fig. 12. Hydrogen bond analysis for the MRSA Penicillin-Binding Protein 2a (PBP2a) complexed with Marmin, a compound isolated from *Citrus australasica* leaves, over 10 ns molecular dynamics simulation. The plot shows the number and stability of hydrogen bonds formed between Marmin and key residues in the PBP2a binding site, indicating consistent hydrogen bonding interactions that contribute to the stability of the protein-ligand complex.

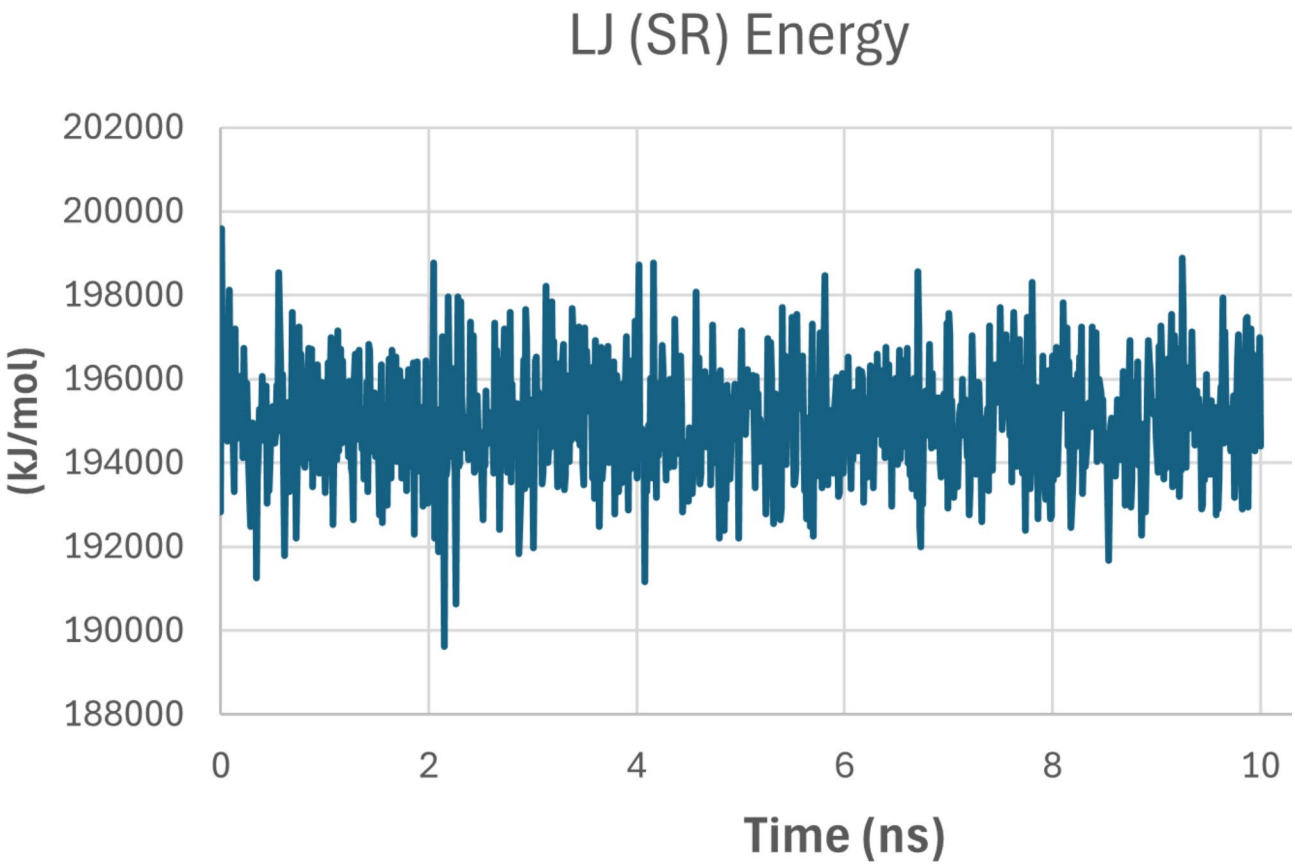

Fig. 13. Lennard-Jones (short-range) energy profile of the MRSA Penicillin-Binding Protein 2a (PBP2a) complexed with Marmin, a compound isolated from *Citrus australasica* leaves, over 10 ns molecular dynamics simulation. The energy profile shows the stability of interactions between Marmin and PBP2a, indicating favorable binding energy contributions that support the potential of Marmin as an effective inhibitor.

Data availability

All data generated or analyzed during this study are included in this published article (and its supplementary information files).

Received: 20 July 2024; Accepted: 24 January 2025
Published online: 20 May 2025

References

1. Cheung, G. Y. C., Bae, J. S. & Otto, M. Pathogenicity and virulence of Staphylococcus aureus. *Virulence* **12**, 547. https://doi.org/10.1080/21505594.2021.1878688 (2021).
2. Ahmed, S. K. et al. Antimicrobial resistance: impacts, challenges, and future prospects. *J. Med. Surg. Public. Health*. **2**, 100081. https://doi.org/10.1016/j.glmedi.2024.100081 (2024).
3. Lakhundi, S. & Zhang, K. Methicillin-Resistant Staphylococcus aureus: molecular characterization, evolution, and Epidemiology. *Clin. Microbiol. Rev.* **31** https://doi.org/10.1128/cmr.00020-18 (2018).
4. Guo, Y., Song, G., Sun, M., Wang, J. & Wang, Y. Prevalence and therapies of antibiotic-resistance in Staphylococcus aureus. *Front. Cell. Infect. Microbiol.* **10**, 107. https://doi.org/10.3389/fcimb.2020.00107 (2020).
5. Sreepian, A., Popruk, S., Nutalai, D., Phutthanu, C. & SreepianP.M. Antibacterial activities and Synergistic Interaction of Citrus essential oils and limonene with gentamicin against clinically isolated Methicillin-Resistant Staphylococcus aureus. *ScientificWorldJournal* **2022** (8418287). https://doi.org/10.1155/2022/8418287 (2022).
6. Parmanik, A. et al. Current treatment strategies against Multidrug-resistant Bacteria: a review. *Curr. Microbiol.* **79**, 388. https://doi.org/10.1007/s00284-022-03061-7 (2022).
7. Shady, N. H. et al. Capturing the antimicrobial profile of Paeonia officinalis, Jasminum officinale and Rosa damascene against methicillin resistant Staphylococcus aureus with metabolomics analysis and network pharmacology. *Sci. Rep.* **14**, 13621. https://doi.org/10.1038/s41598-024-62369-5 (2024).
8. Shady, N. H. et al. Phytochemical analysis and anti-infective potential of fungal endophytes isolated from Nigella sativa seeds. *BMC Microbiol.* **23**, 343. https://doi.org/10.1186/s12866-023-03085-4 (2023).
9. Elmaidomy, A. et al. *Vitis Vinifera Leaves Extract Liposomal Carbopol Gel Preparation's Potential Wound Healing and Anti-MRSA Benefits: In Vivo, Phytochemical, and Computational Investigation*14 (Food & Function, 2023). https://doi.org/10.1039/D2FO03212K
10. Liu, M. et al. Potential of marine natural products against drug-resistant bacterial infections. *Lancet. Infect. Dis.* **19**, e237. https://doi.org/10.1016/S1473-3099(18)30711-4 (2019).

11. Chaudhari, S., Ruknuddin, G. & Prajapati, P. Ethno medicinal values of Citrus Genus: a review. *Med. J. Dr D Y Patil Univ.* **9**, 560. https://doi.org/10.4103/0975-2870.192146 (2016).
12. Santhiya, E. et al. *Phytochemical Anal. Antimicrob. Activity Citrus Lemon Citrus Med.* **11**, 701. (2023).
13. Al-Warhi, T. et al. *Bioactive Phytochemicals of Citrus reticulata Seeds-An Example of Waste Product Rich in Healthy Skin Promoting Agents*. Antioxidants (Basel, Switzerland). 11. (2022). https://doi.org/10.3390/antiox11050984
14. Elmaidomy, A. H. et al. Antiplasmodial potential of phytochemicals from Citrus aurantifolia peels: a comprehensive in vitro and in silico study. *BMC Chem.* **18**, 60. https://doi.org/10.1186/s13065-024-01162-x (2024).
15. Hamilton, K., Ashmore, S. & Drew, R. *Development of Conservation Strategies for Citrus Species of Importance to Australia* (Acta horticulturae, 2005).
16. Rennie, S. *Cultivation of Australian Finger Lime (Citrus australasica)*, in *Australian native plants: cultivation and uses in the health and food industries*. Taylor & Francis London. p. 81. (2017).
17. Delort, E. & Yuan, Y. M. *Finger lime/The Australian Caviar—Citrus australasica, in Exotic Fruits*p. 203 (Elsevier, 2018).
18. Johnson, J. B., Batley, R., Manson, D., White, S. & Naiker, M. Volatile compounds, phenolic acid profiles and phytochemical content of five Australian finger lime (Citrus australasica) cultivars. *LWT* **154**, 112640 (2022).
19. Adhikari, B., Dutt, M. & Vashisth, T. Comparative phytochemical analysis of the fruits of four Florida-grown finger lime (Citrus australasica) selections. *LWT* **135**, 110003 (2021).
20. Lota, M. L., de Rocca Serra, D., Tomi, F., Jacquemond, C. & Casanova, J. Volatile components of peel and leaf oils of lemon and lime species. *J. Agric. Food Chem.* **50**, 796 (2002).
21. Netzel, M., Netzel, G., Tian, Q., Schwartz, S. & Konczak, I. *Native Australian fruits—a Novel Source of Antioxidants for food*8339 (Innovative food science & emerging technologies, 2007).
22. Konczak, I., Zabaras, D., Dunstan, M. & Aguas, P. Antioxidant capacity and hydrophilic phytochemicals in commercially grown native Australian fruits. *Food Chem.* **123**, 1048. https://doi.org/10.1016/j.foodchem.2010.05.060 (2010).
23. Konczak, I. & Roulle, P. Nutritional properties of commercially grown native Australian fruits: lipophilic antioxidants and minerals. *Food Res. Int.* **44**, 2339 (2011).
24. Delort, E. & Jaquier, A. Novel terpenyl esters from Australian finger lime (Citrus australasica) peel extract. *Flavour Fragr. J.* **24**, 123 (2009).
25. Delort, E. et al. Comparative analysis of three Australian finger lime (Citrus australasica) cultivars: identification of unique citrus chemotypes and new volatile molecules. *Phytochemistry* **109**, 111. https://doi.org/10.1016/j.phytochem.2014.10.023 (2015).
26. Ganshirt, H. et al. in *Thin-layer Chromatography; a Laboratory Handbook*. (eds Brenner, M., Bolliger, H. & Stahl, E.) (Springer-, 1965).
27. Elmaidomy, A. H. et al. Antiplasmodial potential of phytochemicals from Citrus aurantifolia peels: a comprehensive in vitro and in silico study. *BMC Chem.* **18**, 60 (2024).
28. Altemani, H. et al. Tamarix aphylla derived metabolites ameliorate indomethacin-induced gastric ulcers in rats by modulating the MAPK signaling pathway, alleviating oxidative stress and inflammation: in vivo study supported by pharmacological network analysis. *Plos One*. **19**, e0302015 (2024).
29. Elmaidomy, A. H. et al. New cytotoxic dammarane type saponins from Ziziphus spina-christi. *Sci. Rep.* **13**, 20612 (2023).
30. Bakhsh, H. T. et al. Anti-alzheimer potential of Solanum lycopersicum seeds: in vitro, in vivo, metabolomic, and computational investigations. *Beni-Suef Univ. J. Basic. Appl. Sci.* **13**, 1 (2024).
31. Elmaidomy, A. H. et al. *Vitis vinifera leaf extract liposomal Carbopol gel preparation's potential wound healing and antibacterial benefits: in vivo, phytochemical, and computational investigation*147156 (Food & Function, 2023).
32. Mohamed, E. M. et al. Anti-alzheimer potential of a New (+)-Pinitol Glycoside isolated from Tamarindus indica pulp: in vivo and in Silico evaluations. *Metabolites* **13**, 732 (2023).
33. Al-Warhi, T. et al. Antioxidant and wound healing potential of Vitis vinifera seeds supported by phytochemical characterization and docking studies. *Antioxidants* **11**, 881 (2022).
34. Elmaidomy, A. H. et al. The anti-alzheimer potential of Tamarindus indica: an in vivo investigation supported by in vitro and in silico approaches. *RSC Adv.* **12**, 11769 (2022).
35. Elmaidomy, A. H. et al. New halogenated compounds from Halimeda macroloba seaweed with potential inhibitory activity against malaria. *Molecules* **27**, 5617 (2022).
36. Bakhsh, H. T. et al. Abelmoschus Eculentus seed extract exhibits in Vitro and in vivo anti-alzheimer's potential supported by Metabolomic and Computational Investigation. *Plants* **12**, 2382 (2023).
37. Alnusaire, T. S. et al. *An in vitro and in silico study of the enhanced antiproliferative and pro-oxidant potential of Olea europaea L. cv. Arbosana leaf extract via elastic nanovesicles (spanlastics)*. Antioxidants. 10, 1860. (2021).
38. Balouiri, M., Sadiki, M. & Ibnsouda, S. K. Methods for in vitro evaluating antimicrobial activity: a review. *J. Pharm. Anal.* **6**, 71. https://doi.org/10.1016/j.jpha.2015.11.005 (2016).
39. Von Mering, C. et al. STRING: known and predicted protein–protein associations, integrated and transferred across organisms. *Nucleic Acids Res.* **33**, D433 (2005).
40. Al-Warhi, T. et al. The wound-healing potential of Olea europaea L. Cv. Arbequina leaves extract: an integrated in vitro, in silico, and in vivo investigation. *Metabolites* **12**, 791 (2022).
41. Zahran, E. M. et al. Scabicidal potential of coconut seed extract in rabbits via downregulating inflammatory/immune cross talk: a comprehensive phytochemical/GC-MS and in silico proof. *Antibiotics* **12**, 43 (2022).
42. Shannon, P. et al. Cytoscape: a software environment for integrated models of biomolecular interaction networks. *Genome Res.* **13**, 2498 (2003).
43. Al-Warhi, T. et al. Bioactive phytochemicals of Citrus reticulata seeds—an example of waste product rich in healthy skin promoting agents. *Antioxidants* **11**, 984 (2022).
44. Bagalagel, A. A. et al. The protective and therapeutic anti-alzheimer potential of Olea europaea L. Cv. Picual: an in silico and in vivo study. *Metabolites* **12**, 1178 (2022).
45. Chin, C. H. et al. cytoHubba: identifying hub objects and sub-networks from complex interactome. *BMC Syst. Biol.* **8** (Suppl 4), S11. https://doi.org/10.1186/1752-0509-8-s4-s11 (2014).
46. Ge, S. X., Jung, D. & Yao, R. ShinyGO: a graphical gene-set enrichment tool for animals and plants. *Bioinf. (Oxford England)*. **36**, 2628. https://doi.org/10.1093/bioinformatics/btz931 (2020).
47. Tang, D. et al. SRplot: a free online platform for data visualization and graphing. *PloS One*. **18**, e0294236. https://doi.org/10.1371/journal.pone.0294236 (2023).
48. Pettersen, E. F. et al. UCSF ChimeraX: structure visualization for researchers, educators, and developers. *Protein Sci.* **30**, 70 (2021).
49. Farid, N., Bux, K., Ali, K., Bashir, A. & Tahir, R. Repurposing amphotericin B: anti-microbial, molecular docking and molecular dynamics simulation studies suggest inhibition potential of amphotericin B against MRSA. *BMC Chem.* **17**, 67 (2023).
50. Studio, D. *Discovery studio*. Accelrys [2.1]. (2008).
51. Musa, A. et al. *Cytotoxic potential, metabolic profiling, and liposomes of Coscinoderma sp. crude extract supported by in silico analysis*. *Int. J. Nanomed.* 20213861 .
52. Elmaidomy, A. H. et al. Acylated iridoids and rhamnopyranoses from premna odorata (lamiaceae) as novel mesenchymal–epithelial transition factor receptor inhibitors for the control of breast cancer. *Phytother. Res.* **31**, 1546 (2017).
53. Alzarea, S. I. et al. Potential anticancer lipoxygenase inhibitors from the red sea-derived brown algae sargassum cinereum: an in-silico-supported In-Vitro Study. *Antibiotics* **10**, 416 (2021).

54. Shamikh, Y. I. et al. Actinomycetes from the Red Sea sponge Coscinoderma mathewsi: isolation, diversity, and potential for bioactive compounds discovery. *Microorganisms* **8**, 783 (2020).
55. Vieira, I. H. P. et al. Visual dynamics: a web application for molecular dynamics simulation using GROMACS. *BMC Bioinform.* **24**, 107 (2023).
56. Beu, T. A. & Farcaş, A. CHARMM force field and molecular dynamics simulations of protonated polyethylenimine. *J. Comput. Chem.* **38**, 2335 (2017).
57. Chinchansure, A., Shamnani, N., Arkile, M., Sarkar, D. & Joshi, S. Antimycobacterium activity of coumarins from fruit pulp of Aegle marmelos (l.) Correa. *Int. J. Basic. Appl. Chem. Sci.* **5**, 39 (2015).
58. Khan, A. J., Kunesch, G., Chuilon, S. & Ravise, A. Structure and biological activity of xanthyletin, a new phytoalexin of citrus. *Fruits* **40**, 807 (1985).
59. Zor, M., Aydin, S., Güner, N. D., Başaran, N. & Başaran, A. A. Antigenotoxic properties of Paliurus spina-christi Mill fruits and their active compounds. *BMC Complement. Altern. Med.* **17**, 1 (2017).
60. Lee, E. H. et al. Constituents of the stems and fruits of Opuntia ficus-indica var. Saboten. *Arch. Pharm. Res.* **26**, 1018 (2003).
61. Xiao, H. et al. *Isolation and characterization of plant-based lactic acid bacteria from spontaneously fermented foods using a new modified medium*. LWT. 2023115695.
62. Zhang, B. L., Buddrus, S., Trierweiler, M. & Martin, G. J. Characterization of glycerol from different origins by 2H-and 13 C-NMR studies of site-specific natural isotope fractionation. *J. Agric. Food Chem.* **46**, 1374 (1998).
63. Aliba, M., Ndukwe, I. & Ibrahim, H. Isolation and characterization of B-sitosterol from methanol extracts of the stem bark of large-leaved rock fig (Ficus Abutilifolia Miq). *J. Appl. Sci. Environ. Manage.* **22**, 1639 (2018).
64. Kanehisa, M. & Goto, S. KEGG: kyoto encyclopedia of genes and genomes. *Nucleic Acids Res.* **28**, 27. https://doi.org/10.1093/nar/28.1.27 (2000).
65. Kanehisa, M. Toward understanding the origin and evolution of cellular organisms. *Protein Science: Publication Protein Soc.* **28**, 1947. https://doi.org/10.1002/pro.3715 (2019).
66. Kanehisa, M., Furumichi, M., Sato, Y., Kawashima, M. & Ishiguro-Watanabe, M. KEGG for taxonomy-based analysis of pathways and genomes. *Nucleic Acids Res.* **51**, D587. https://doi.org/10.1093/nar/gkac963 (2023).
67. Kwatra, B., Khatun, A., Bhowmik, R. & Rehman, S. In silico-modelling of phytochemicals in septic arthritis. *Pharma Innov.* **10**, 14 (2021).
68. Lim, D. & Strynadka, N. C. Structural basis for the β lactam resistance of PBP2a from methicillin-resistant Staphylococcus aureus. *Nat. Struct. Biol.* **9**, 870 (2002).
69. Rosignoli, S. & Paiardini, A. Boosting the full potential of PyMOL with structural biology plugins. *Biomolecules* **12**, 1764 (2022).

Acknowledgements

The authors thank the Deanship of Scientific Research at King Khalid University for funding this work through a small group Research Project under grant number RGP1/192/45.

Author contributions

Conceptualization: URA, MAZ; methodology: AHE, EMM, SMF, RIB, GMA; software; Formal analysis: AHE, EMM, HAA; investigation: URA, MAZ, HAA; writing—original draft: All authors; writing—review and editing: all authors; supervision: URA, MAZ, RIB. All authors have read and agreed to the published version of the manuscript.

Declarations

Competing interests

The authors declare no competing interests.

Additional information

Supplementary Information The online version contains supplementary material available at https://doi.org/10.1038/s41598-025-88113-1.

Correspondence and requests for materials should be addressed to G.M.A. or U.R.A.